Distributed QC-LDPC Coded Spatial Modulation for Half-Duplex Wireless Communications

Chunli ZHAO [1], Fengfan YANG [1], Daniel Kariuki WAWERU [1], Chen CHEN [1], Hongjun XU [2]

[1] College of Electronics and Information Engg., Nanjing Univ. of Aeronautics and Astronautics, Nanjing, 210016 China
[2] School of Engineering, University of KwaZulu-Natal, King George V Avenue, Durban, 4041, South Africa

chunlizhao_cn@163.com, yffee@nuaa.edu.cn, daniel.kariuki19@nuaa.edu.cn, chen_chen0518@163.com, xuh@ukzn.ac.za

Submitted January 16, 2022 / Accepted July 9, 2022 / Online first August 3, 2022

Abstract. *The bit error rate (BER) performance of spatial modulation (SM) can be further improved by applying quasi-cyclic low-density parity-check (QC-LDPC) codes recommended in 5G to SM. It motivates us to propose a QC-LDPC coded SM (QC-LDPCC-SM) scheme, where SM signals are protected by QC-LDPC codes. To estimate the channel state information at the receiver, a novel iterative joint channel estimation and data detection based on variable block length (IJCEDD-VBL) for SM is presented. In standard 5G LDPC codes, the parity-check matrix contains multiple submatrices, and then we can construct two different QC-LDPC codes by suitably selecting the submatrices. Thus, the QC-LDPCC-SM scheme can be effectively extended to cooperative scenarios when deploying the generated LDPC codes at the source and relay, respectively. We develop an analytical approach for the BER performance of the proposed schemes. The simulation and theoretical results are in good agreement at high signal-to-noise ratio (SNR). Furthermore, the proposed coded cooperative scheme outperforms its corresponding non-cooperative counterpart and the existing scheme. The numerical results also validate the effectiveness of the proposed channel estimation scheme.*

Keywords

Quasi-Cyclic Low-Density Parity-Check (QC-LDPC) codes, coded cooperation, Spatial Modulation (SM), half-duplex

1. Introduction

Channel coding is a key communication technology for guaranteeing the reliable transmission through error control. As a kind of capacity-approaching channel codes, low-density parity-check (LDPC) codes have been widely explored and applied in different practical communication systems [1]. In terms of LDPC codes, their structure and performance are defined by the parity-check matrices, thus a key to designing LDPC codes is to construct the parity-check matrices. In general, the parity-check matrices are constructed by random-like or structured methods. On the basis of the construction methods, LDPC codes are roughly divided into random-like LDPC codes and structured LDPC codes. It is well known that quasi-cyclic LDPC (QC-LDPC) codes [2] are recognized as a special kind of structured LDPC codes. Different from random-like LDPC codes, the parity-check matrices of QC-LDPC codes are comprised of multiple square matrices with the same size, where each square matrix is a circularly-shifted identity matrix or zero matrix. It is very convenient for the storage and addressing of the memory, thus greatly reducing the encoding and decoding complexity. Furthermore, QC-LDPC codes with repeated accumulation structure can implement fast encoding [3] and achieve good performance. Due to many advantages of QC-LDPC codes, they have been recommended by Third Generation Partnership Project (3GPP) as the encoding method for 5G new radio (NR).

Coded cooperation as a combination of cooperative schemes and channel coding is a technique that effectively combats the channel impairments [4], [5]. There are three basic relaying techniques, i.e., amplify-and-forward (AF) [6], decode-and-forward (DF) [7] and compress-and-forward (CF) [8]. In the AF, the relay directly sends an amplified version of the information received from the transmitter to the destination. In the DF, the relay decodes the received signal from the source, re-encodes and then transmits the re-encoded symbols to the destination. In the CF, the relay node gets the message from the source and sends a compressed version of it to the destination. Thus, the DF relaying technique is the most realistic relaying scheme that counters the effect of noise in the relay among the three relaying protocols, especially when the source to relay link is good. Therefore, we employ the DF protocol in this paper. In a coded cooperative scheme, a distributed channel code is formed at the destination node through the mutual cooperation between source and relay nodes. Recently, different distributed channel coding schemes such as distributed turbo codes [8], distributed LDPC codes [7], distributed Reed-Muller codes [9] and distributed polar codes [10] have been reported.

DOI: 10.13164/re.2022.0362

Multiple-input multiple-output (MIMO) techniques are also promising technologies that resist the channel fading. Spatial modulation (SM) [11] as a recently developed MIMO transmission technique is attracting attention. It is because SM has a significant feature, i.e., at each time instant a single active transmitting antenna propagates symbols taken from constellation diagram, which efficiently avoids the inter-channel interference (ICI) and inter-antenna synchronization (IAS) [11], [12]. Many related literatures such as [13–15] have reported the coded SM schemes, and they also present that incorporating SM into channel coding can achieve a good performance. Motivated by this, we investigate the QC-LDPC coded SM (QC-LDPCC-SM) as the amalgamation of the new channel coding technique (5G LDPC codes) and SM. Usually in practical communication systems, the receiver has imperfect channel state information (CSI). Therefore, we propose a novel iterative joint channel estimation (CE) and data detection (DD) based on variable block length (IJCEDD-VBL) for SM, to estimate the CSI. In 5G LDPC codes, their parity-check matrices contain multiple submatrices. By properly choosing the submatrices to generate two different QC-LDPC codes utilized at source and relay, respectively, we can efficiently extend the QC-LDPCC-SM to cooperative scenarios, i.e., distributed QC-LDPC coded SM (D-QC-LDPCC-SM). Moreover, for 5G LDPC codes, two base matrices are accepted and each base matrix has eight exponent matrices [2]. Based on the information length and code rate, the base matrix and cyclic shifts (the elements of exponent matrix) can be determined by using the method in [1]. Then, we can obtain the parity-check matrix with the help of the base matrix and exponent matrix. The generated parity-check matrix is easy to avoid the appearance of short cycles so that the length of the shortest cycle is as large as possible, which can efficiently improve the performance of proposed coded cooperative and non-cooperative schemes.

Due to the maturity and low cost of half-duplex relay, it is very convenient and popular to be used in our proposed D-QC-LDPCC-SM scheme. Also, adopting the half-duplex strategy can avoid interference between the two orthogonal time slots. When employing the half-duplex strategy, the joint decoder in the destination can easily retrieve the message conveyed in the source by jointly decoding the source and relay sequences generated at the two orthogonal slots. Thus, the half-duplex relay is utilized in our proposed D-QC-LDPCC-SM.

The main contributions of this article are as follows:

- We propose the QC-LDPCC-SM scheme in non-cooperative scenarios. A new IJCEDD-VBL scheme is developed to estimate the CSI.
- We effectively extend the QC-LDPCC-SM scheme to half-duplex cooperative communication scenarios with a single relay, i.e., D-QC-LDPCC-SM scheme.
- We derive and validate the theoretical performance bound of the proposed schemes.
- We investigate the error performance of the proposed D-QC-LDPCC-SM in realistic channel scenarios, i.e., non-ideal source-to-relay channel. Additionally, we discuss the performance of the QC-LDPCC-SM scheme under correlated channel conditions.

The rest of this manuscript is organized as follows. We present the features of 5G LDPC codes in Sec. 2. The QC-LDPCC-SM is elaborated in Sec. 3. Furthermore, Section 4 describes the D-QC-LDPCC-SM scheme. Section 5 performs the analytical calculation of bit error rate (BER) for the proposed schemes. Section 6 provides the simulation results of the investigated schemes. Finally, Section 7 concludes this manuscript.

2. Features of 5G LDPC Codes

A QC-LDPC code is defined by its parity-check matrix including circularly-shifted identity matrices and zero matrices, with the same size $Z \times Z$. The parity-check matrix is

$$\mathbf{H}_0 = \begin{bmatrix} \mathbf{M}^{p_{1,1}} & \mathbf{M}^{p_{1,2}} & \mathbf{M}^{p_{1,3}} & \cdots & \mathbf{M}^{p_{1,n_\mathrm{b}}} \\ \mathbf{M}^{p_{2,1}} & \mathbf{M}^{p_{2,2}} & \mathbf{M}^{p_{2,3}} & \cdots & \mathbf{M}^{p_{2,n_\mathrm{b}}} \\ \vdots & \vdots & \vdots & \ddots & \vdots \\ \mathbf{M}^{p_{m_\mathrm{b},1}} & \mathbf{M}^{p_{m_\mathrm{b},2}} & \mathbf{M}^{p_{m_\mathrm{b},3}} & \cdots & \mathbf{M}^{p_{m_\mathrm{b},n_\mathrm{b}}} \end{bmatrix} \tag{1}$$

where Z is the lifting size. $\mathbf{M}$ is a $Z \times Z$ standard permutation matrix, i.e., cyclically shifted identity matrix (a non-negative power denotes the shift value), and denoted as

$$\mathbf{M} = \begin{bmatrix} 0 & 1 & 0 & \cdots & 0 \\ 0 & 0 & 1 & \cdots & 0 \\ \vdots & \vdots & \vdots & \vdots & \vdots \\ 0 & 0 & 0 & \ddots & 1 \\ 1 & 0 & 0 & \cdots & 0 \end{bmatrix}. \tag{2}$$

Also, $p_{i,j} \in \{-1, 0, ..., Z-1\}$ for $1 \le i \le m_\mathrm{b}$, $1 \le j \le n_\mathrm{b}$. If $p_{i,j} = -1$, $\mathbf{M}^{p_{i,j}} = \mathbf{0}$ ($\mathbf{0}$ is all-zero matrix), and if $p_{i,j} \neq -1$, $\mathbf{M}^{p_{i,j}} = (\mathbf{M})^{p_{i,j}}$. All the shifts form the following matrix

$$\mathbf{P} = \begin{bmatrix} p_{1,1} & p_{1,2} & p_{1,3} & \cdots & p_{1,n_\mathrm{b}} \\ p_{2,1} & p_{2,2} & p_{2,3} & \cdots & p_{2,n_\mathrm{b}} \\ \vdots & \vdots & \vdots & \ddots & \vdots \\ p_{m_\mathrm{b},1} & p_{m_\mathrm{b},2} & p_{m_\mathrm{b},3} & \cdots & p_{m_\mathrm{b},n_\mathrm{b}} \end{bmatrix}. \tag{3}$$

We observe that the parity-check matrix $\mathbf{H}_0$ is formed from the matrix $\mathbf{P}$. Here, the matrix $\mathbf{P}$ is called the exponent matrix of $\mathbf{H}_0$. Then, the base matrix $\mathbf{B}$ is defined as

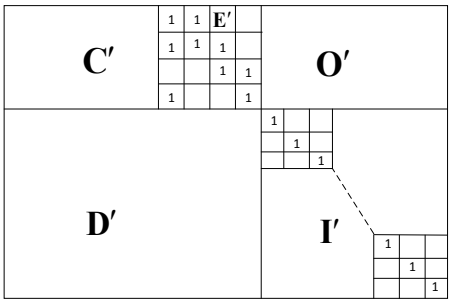

Fig. 1. Basic sketch of base matrix for 5G LDPC codes.

$$\mathbf{B}=\begin{bmatrix} b_{1,1} & b_{1,2} & b_{1,3} & \cdots & b_{1,n_b} \\ b_{2,1} & b_{2,2} & b_{2,3} & \cdots & b_{2,n_b} \\ \vdots & \vdots & \vdots & \ddots & \vdots \\ b_{m_b,1} & b_{m_b,2} & b_{m_b,3} & \cdots & b_{m_b,n_b} \end{bmatrix} \tag{4}$$

where $b_{i,j}=0$ if $p_{i,j}=-1$ and $b_{i,j}=1$ otherwise.

Figure 1 depicts the basic sketch of base matrix for 5G LDPC codes. The base matrix contains submatrices $\mathbf{C}'$, $\mathbf{E}'$, $\mathbf{O}'$, $\mathbf{D}'$ and $\mathbf{I}'$ of sizes $4\times k_b$, 4×4, $4\times(m_b-4)$, $(m_b-4)\times(k_b+4)$ and $(m_b-4)\times(m_b-4)$, respectively, where $k_b+m_b=n_b$. The submatrices $\mathbf{C}'$ and $\mathbf{E}'$ form the core, while the remaining submatrices $\mathbf{O}'$, $\mathbf{D}'$ and $\mathbf{I}'$ together form extensions. Moreover, $\mathbf{O}'$ and $\mathbf{I}'$ stand for zero and identity matrices, respectively. Submatrix $\mathbf{E}'$ denotes a square matrix and has a particularly interesting structure, in which the first column is of weight 3 and the remaining columns jointly constitute a bidiagonal structure. The submatrices $\mathbf{C}'$, $\mathbf{E}'$ and $\mathbf{I}'$ separately correspond to systematic information sequence, the first and second parts of parity-check sequences. Obviously, this construction is like Raptor-like extension [16].

In 5G LDPC codes, two base matrices ($\mathbf{B}_1$ of 46 × 68 and $\mathbf{B}_2$ of 42 × 52) are supported. As introduced in [2], $\mathbf{B}_1$ and $\mathbf{B}_2$ possess similar structures. In this article, the authors concentrate on $\mathbf{B}_1$ of 46 × 68 ($m_b=46$, $n_b=68$, $k_b=22$) designed for message lengths ($500\le K\le 8448$) and code rates ($1/3\le R_c\le 8/9$). This design of exponent matrix depends on the base matrix and shift values, and the reader can refer to [1] to study the detailed design steps of exponent matrix. By dispersing every element of the exponent matrix into a $Z\times Z$ circularly-shifted identity matrix or zero matrix, the parity-check matrix $\mathbf{H}_0$ will be obtained, and denoted as [1]

$$\mathbf{H}_0=\begin{bmatrix} \mathbf{C} & \mathbf{E} & \mathbf{O} \\ \mathbf{D}_1 & \mathbf{D}_2 & \mathbf{I} \end{bmatrix} \tag{5}$$

where the sizes of $\mathbf{C}$, $\mathbf{E}$, $\mathbf{D}_1$ and $\mathbf{D}_2$ are $4Z\times k_bZ$, $4Z\times 4Z$, $(m_b-4)Z\times k_bZ$ and $(m_b-4)Z\times 4Z$, respectively. Furthermore, $\mathbf{O}$ is a $4Z\times(m_b-4)Z$ zero matrix and $\mathbf{I}$ is a $(m_b-4)Z\times(m_b-4)Z$ identity matrix.

By using this designed base matrix, the approximate performance can be analyzed by using the performance estimation tool. Furthermore, for the elements 1s in the base matrix, by designing specific shift values the parity-check matrix is then obtained. Therefore, this implies that the base matrix is the product of the intermediate process of designing the parity-check matrix, and plays an indispensable role in the communication system operating based on QC-LDPC codes.

3. QC-LDPC Coded SM Scheme

We discuss the coded SM scheme with 5G LDPC codes in this section. Firstly, we introduce the system model of the QC-LDPCC-SM scheme. Then, we present the proposed IJCEDD-VBL scheme to estimate the CSI.

3.1 System Model

The system model is described in Fig. 2, where N_T transmitting antennas and N_R receiving antennas are used. At the source (S), the sequence $\mathbf{u}'$ is encoded into code sequence $\mathbf{c}$ by the (N,K) QC-LDPC encoder (we focus on the code with low code rate $R_c=K/N=1/3$ in this paper). Specifically, $\mathbf{u}'$ is first expanded into $\mathbf{u}$ with k_bZ bits by the zero padding block. The resulted $\mathbf{u}$ is encoded into a code sequence $\mathbf{c}'$ of length n_bZ after the 5G LDPC encoding block with the parity-check matrix $\mathbf{H}_0$ shown in (5). Through the zero removing and puncturing block, the transmitted code sequence $\mathbf{c}$ with length N is produced. Figure 3 gives an explanation for the encoding process. The bit grouping block then takes the sequence $\mathbf{c}$ and splits it into $\mathbf{c}(\tau)$ with length $d=\log_2(N_TM)$ for $\tau=1,2,...,L=(N+\bar{N})/d$, in which M stands for the modulation order and $\bar{N}$ represents the number of dummy bits appended at the end of $\mathbf{c}$ such that its length becomes an integer multiple of d. The generated sequence $\mathbf{c}(\tau)$ enters the SM mapper that consists of the bit divider, antenna modulator, M-ary digital modulator and coded spatial modulator. Among them, the bit divider accepts $\mathbf{c}(\tau)$ and partitions it into $\mathbf{c}_1(\tau)$ and $\mathbf{c}_2(\tau)$ of lengths $x=\log_2(N_T)$ and $y=\log_2(M)$, respectively. The antenna modulator gets the first part $\mathbf{c}_1(\tau)$ to specify an antenna index labelled by $a(\tau)\in\{1,2,...,N_T\}$. The remaining $\mathbf{c}_2(\tau)$ is given into the digital modulator (using Gray mapping) generating the modulated symbol $c_m(\tau)$ taken from M possible constellation points, where $m\in\{1,2,...,M\}$. The constellation symbol $c_m(\tau)$ is conveyed at the $a(\tau)$-th transmit antenna and then the coded spatial modulator outputs the $N_T\times 1$ dimensional transmission vector [17]

$$\mathbf{c}_{m,a}(\tau)=[...,0,c_m(\tau),0,...]^T \tag{6}$$

where only the element at the $a(\tau)$-th position is non-zero, and $[.]^T$ represents the transpose operator. In the following, the vector $\mathbf{c}_{m,a}(\tau)$ is propagated via quasi-static Rayleigh fading channel $\mathbf{H}\in\mathbb{C}^{N_R\times N_T}$ with the additive Gaus-

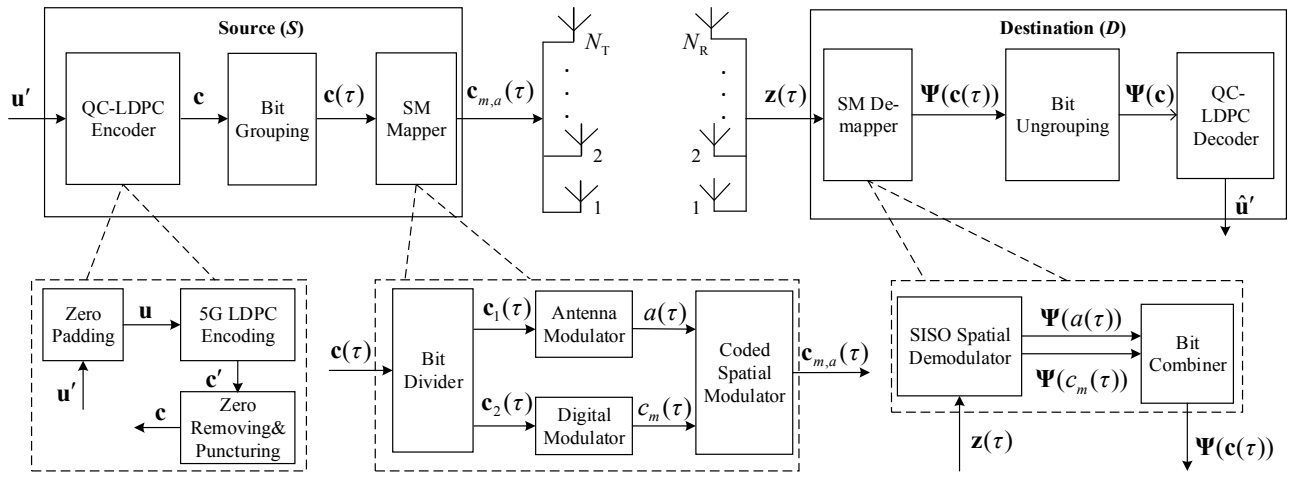

Fig. 2. System model of the QC-LDPCC-SM scheme in non-cooperative scenarios.

sian noise $\mathbf{n}(\tau) \in \mathbb{C}^{N_R \times 1}$, where $\mathbb{C}$ denotes the complex domain. For $\mathbf{H}$, all the entries follow the complex Gaussian distribution $CN(0,1)$ with zero mean and unit variance. Likewise, each element in the noise vector $\mathbf{n}(\tau) \in \mathbb{C}^{N_R \times 1}$ obeys the complex Gaussian distribution $CN(0, N_0)$. At the destination (D), the received sequence $\mathbf{z}(\tau) \in \mathbb{C}^{N_R \times 1}$ is

$$\mathbf{z}(\tau) = \mathbf{H}\mathbf{c}_{m,a}(\tau) + \mathbf{n}(\tau) = \mathbf{h}^{a(\tau)} c_m(\tau) + \mathbf{n}(\tau) \qquad (7)$$

where $\mathbf{h}^{a(\tau)} \in \mathbb{C}^{N_R \times 1}$ denotes the $a(\tau)$-th column of $\mathbf{H}$. Soft-input soft-output (SISO) spatial demodulator using maximum-likelihood detection (MLD) [15] gets $\mathbf{z}(\tau)$ and generates log-likelihood ratios (LLRs) $\mathbf{\Psi}(a(\tau))$ and $\mathbf{\Psi}(c_m(\tau))$ corresponding to $a(\tau)$ and $c_m(\tau)$, respectively. To know it well, Table 1 shows the mapping procedure for SM, where Gray mapping is utilized for modulation. The sequence $\mathbf{c}(\tau)$ of length $d = \log_2(N_T M) = 3$ is considered. As compared to conventional digital modulation schemes (such as amplitude-shift-keying (ASK)), phase-shift-keying (PSK) and quadrature amplitude modulation (QAM) have stronger anti-noise capabilities and are more adaptive to the

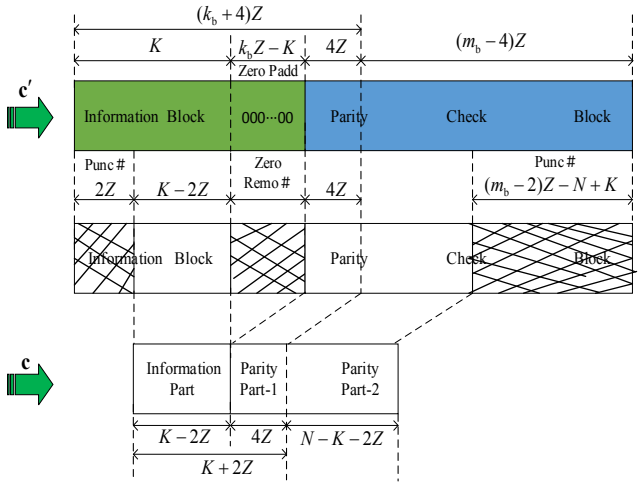

Fig. 3. Zero padding, puncturing and zero removing of standard 5G LDPC codes.

Sequence $\mathbf{c}(\tau)$	$N_T = 2$, 4-QAM	$N_T = 4$, BPSK
	$(a(\tau), c_m(\tau))$	$(a(\tau), c_m(\tau))$
[0, 0, 0]	(1, – 1 – i)	(1, – 1)
[0, 0, 1]	(1, – 1 + i)	(1, + 1)
[0, 1, 0]	(1, + 1 – i)	(2, – 1)
[0, 1, 1]	(1, + 1 + i)	(2, + 1)
[1, 0, 0]	(2, – 1 – i)	(3, – 1)
[1, 0, 1]	(2, – 1 + i)	(3, + 1)
[1, 1, 0]	(2, + 1 – i)	(4, – 1)
[1, 1, 1]	(2, + 1 + i)	(4, + 1)

Tab. 1. Mapping process for SM with LDPC codes.

channel change [18]. Thus, we adopt the two scenarios, i.e., the combination of $N_T = 2$ and 4-QAM (4-PSK), and the combination of $N_T = 4$ and binary PSK (BPSK). For the sequence $\mathbf{c}(\tau)$ the first $\log_2(N_T)$ antenna bits and the remaining $\log_2(M)$ symbol bits are mapped to the antenna index $a(\tau) \in \{1,2,\ldots,N_T\}$ and the constellation symbol $c_m(\tau)$, respectively. The rule shows that the mapping procedures of each scenario are not unique. For example, for the first scenario, the antenna bits 0 and 1 can be mapped to the antenna indices 2 and 1, respectively. The symbol bits [0, 0], [0, 1], [1, 0] and [1, 1] can be mapped to the symbols + 1 + i, + 1 – i, – 1 + i and – 1 – i, respectively. However, for each mapping procedure of each scenario, the minimum Euclidean distance between two different SM transmit vectors is identical. Thus, different procedures in each scenario result in almost the same error performance. Then, we only list one procedure for each scenario.

After the bit combiner, we obtain the sequence $\mathbf{\Psi}(\mathbf{c}(\tau)) = [\mathbf{\Psi}(a(\tau)), \mathbf{\Psi}(c_m(\tau))]$ which is merged into $\mathbf{\Psi}(\mathbf{c})$ by the bit ungrouping. Finally, the QC-LDPC decoder provides an estimation $\hat{\mathbf{u}}'$ for $\mathbf{u}'$ on the basis of Tanner graph corresponding to the parity-check matrix $\mathbf{H}_0$. Note that the filler zero bits and the punctured check bits do not participate in the realistic channel transmission. Therefore,

in the LDPC decoding, we don't need to update the extrinsic information corresponding to these bits, which can reduce the decoding delay.

3.2 Proposed Iterative Joint CE and DD Based on Variable Block Length

In realistic communication systems, the receiver usually has imperfect CSI. To accurately estimate the CSI, it is necessary to reduce the influence of CE errors. In this section, we propose a novel IJCEDD-VBL scheme for SM, where minimum mean square error (MMSE) CE and MLD are used. The closest work related to our proposed scheme is iterative joint CE and DD (IJCEDD) presented in [17]. However, in [17], the whole frame rather than block-by-block signals are detected, which results in error propagation.

In the proposed IJCEDD-VBL, we partition L SM symbols at the destination into J blocks. Thus, each block has $T = L/J$ symbols. Furthermore, the IJCEDD is employed in each block, where the estimated CSI in the j-th block and in the i-th iteration is denoted as $\hat{\mathbf{H}}_{j,i}$ ($1 \le j \le J$, $1 \le i \le I_{\text{itr}}$). However, the CSI estimated by the training SM symbol block is represented as $\hat{\mathbf{H}}_{0,I_{\text{itr}}}$. With the aid of the MMSE criterion, the CSI $\hat{\mathbf{H}}_{0,I_{\text{itr}}} \in \mathbb{C}^{N_{\text{R}} \times N_{\text{T}}}$ is expressed as

$$\hat{\mathbf{H}}_{0,I_{\text{itr}}} = \mathbf{Z}_0(\mathbf{Q}_0^{\text{H}}\mathbf{R}_{\mathbf{H}}\mathbf{Q}_0 + N_0 N_{\text{R}}\mathbf{I}_{T\times T})^{-1}\mathbf{Q}_0^{\text{H}}\mathbf{R}_{\mathbf{H}} \quad (8)$$

where $\mathbf{Q}_0 \in \mathbb{C}^{N_{\text{T}}\times T}$ is the training symbol block, $\mathbf{Z}_0 \in \mathbb{C}^{N_{\text{R}}\times T}$ is the received training signal block corresponding to $\mathbf{Q}_0$, $(.)^{\text{H}}$ is the Hermitian transpose, $\mathbf{I}_{T\times T}$ is the identity matrix of size $T \times T$, $(.)^{-1}$ is the inverse operation and $\mathbf{R}_{\mathbf{H}} = E[\mathbf{H}^{\text{H}}\mathbf{H}] \in \mathbb{C}^{N_{\text{T}}\times N_{\text{T}}}$ is the channel's correlation matrix with $E[.]$ denoting the expectation operator.

For ensuring to efficiently low the effects of CE errors, we take the CSI $\hat{\mathbf{H}}_{j-1,I_{\text{itr}}}$ estimated in the previous $(j-1)$-th block as the initial CSI $\hat{\mathbf{H}}_{j,0}$ of the current j-th block. In the i-th iteration of the j-th block, the SM symbols $\hat{\mathbf{c}}_{m,a}^{j,i}(\tau) \in \mathbb{C}^{N_{\text{T}}\times 1}$ are detected by utilizing MLD as follows:

$$\hat{\mathbf{c}}_{m,a}^{j,i}(t) = \arg\min_{\mathbf{c}_{m,a}(t)} \| \mathbf{z}((j-1)T+t) - \hat{\mathbf{H}}_{j,i-1}\mathbf{c}_{m,a}(t) \|_{\text{F}}^2 \quad (9)$$

where $t \in \{1,2,...,T\}$ and $\|.\|_{\text{F}}$ is the Frobenius norm. Based on (9), we get the concatenated detected symbol block denoted as

$$\hat{\mathbf{Q}}_{j,i} = [\hat{\mathbf{c}}_{m,a}^{j,i}((j-1)T+1), \hat{\mathbf{c}}_{m,a}^{j,i}((j-1)T+2), ..., \hat{\mathbf{c}}_{m,a}^{j,i}(jT)]. \quad (10)$$

According to the generated $\hat{\mathbf{Q}}_{j,i}$ in (10), the updated estimated CSI $\hat{\mathbf{H}}_{j,i} \in \mathbb{C}^{N_{\text{R}}\times N_{\text{T}}}$ is given by

$$\hat{\mathbf{H}}_{j,i} = \mathbf{Z}_j(\hat{\mathbf{Q}}_{j,i}^{\text{H}}\mathbf{R}_{\mathbf{H}}\hat{\mathbf{Q}}_{j,i} + N_0 N_{\text{R}}\mathbf{I}_{T\times T})^{-1}\hat{\mathbf{Q}}_{j,i}^{\text{H}}\mathbf{R}_{\mathbf{H}} \quad (11)$$

Algorithm 1 The proposed IJCEDD-VBL

Input: $\mathbf{Z}_0$, $\mathbf{Q}_0$, $\mathbf{R}_{\mathbf{H}}$, N_0, N_{R}, $\mathbf{I}_{T\times T}$, J, I_{itr}, T.

Output: $\hat{\mathbf{H}}_{J,I_{\text{itr}}}$.

1: Set $\hat{\mathbf{H}}_{0,I_{\text{itr}}} = \mathbf{Z}_0(\mathbf{Q}_0^{\text{H}}\mathbf{R}_{\mathbf{H}}\mathbf{Q}_0 + N_0 N_{\text{R}}\mathbf{I}_{T\times T})^{-1}\mathbf{Q}_0^{\text{H}}\mathbf{R}_{\mathbf{H}}$.

2: **for** j=1 to J **do**

3: $\hat{\mathbf{H}}_{j,0} = \hat{\mathbf{H}}_{j-1,I_{\text{itr}}}$.

4: **for** i=1 to I_{itr} **do**

5: **for** t=1 to T **do**

6: Perform the MLD on the received signals and yield $\hat{\mathbf{c}}_{m,a}^{j,i}(t) = \arg\min_{\mathbf{c}_{m,a}(t)} \| \mathbf{z}((j-1)T+t) - \hat{\mathbf{H}}_{j,i-1}\mathbf{c}_{m,a}(t) \|_{\text{F}}^2$.

7: **end for**

8: Based on the detected SM symbols, get the concatenated estimated symbol block: $\hat{\mathbf{Q}}_{j,i} = [\hat{\mathbf{c}}_{m,a}^{j,i}((j-1)T+1), \hat{\mathbf{c}}_{m,a}^{j,i}((j-1)T+2), ..., \hat{\mathbf{c}}_{m,a}^{j,i}(jT)]$.

9: Update the CSI by employing the following expression: $\hat{\mathbf{H}}_{j,i} = \mathbf{Z}_j(\hat{\mathbf{Q}}_{j,i}^{\text{H}}\mathbf{R}_{\mathbf{H}}\hat{\mathbf{Q}}_{j,i} + N_0 N_{\text{R}}\mathbf{I}_{T\times T})^{-1}\hat{\mathbf{Q}}_{j,i}^{\text{H}}\mathbf{R}_{\mathbf{H}}$.

10: **end for**

11: **end for**

Tab. 2. Generation process of estimated channel.

where the received signal block $\mathbf{Z}_j \in \mathbb{C}^{N_{\text{R}}\times T}$ is written as the following form:

$$\mathbf{Z}_j = [\mathbf{z}((j-1)T+1), \mathbf{z}((j-1)T+2), ..., \mathbf{z}(jT)]. \quad (12)$$

Repeat (9) and (11) until the number of iterations reaches I_{itr}. Finally, the estimated CSI $\hat{\mathbf{H}} = \hat{\mathbf{H}}_{J,I_{\text{itr}}}$ is obtained. The generated process of the estimated CSI is illustrated in Algorithm 1 of Tab. 2.

4. Distributed QC-LDPC Coded SM Scheme

The QC-LDPCC-SM scheme can be efficiently extended to cooperative scenarios by appropriately choosing the submatrices in (5) to generate two different QC-LDPC codes utilized at S and relay (R), respectively. The proposed D-QC-LDPCC-SM scheme over quasi-static Rayleigh fading channel is observed in Fig. 4, where the parity-check matrices at S and R are denoted as $\mathbf{H}_1 = [\mathbf{C}, \mathbf{E}]$ and $\mathbf{H}_2 = [\mathbf{D}_1, \mathbf{D}_2, \mathbf{I}]$, respectively. It takes two time slots for a whole coded cooperative communication transmission.

In time slot-1, the information sequence $\mathbf{u}'$ with K bits at the source is updated into $\mathbf{u}$ of length $k_{\text{b}}Z$ through the zero padding block. After the QC-LDPC$_1$ encoding with the parity-check matrix $\mathbf{H}_1 = [\mathbf{C}, \mathbf{E}]$, we get the code sequence $\mathbf{c}'^S$ of length $(k_{\text{b}}+4)Z$. By the zero removing and puncturing block, $\mathbf{c}'^S$ is transformed into the sequence $\mathbf{c}^S$ of length $N_1 = K + 2Z$, where $\mathbf{c}^S$ includes the information part of length $K - 2Z$ and parity part-1 of length $4Z$

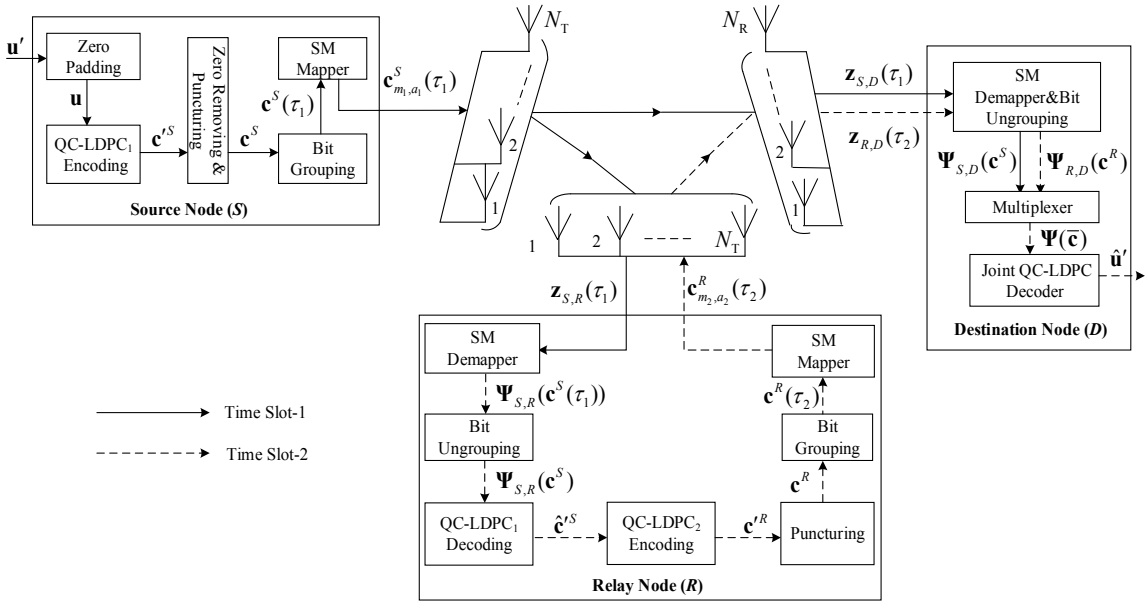

Fig. 4. D-QC-LDPCC-SM scheme for cooperative communications.

shown in Fig. 3. Next, $\mathbf{c}^S$ is divided into $\mathbf{c}^S(\tau_1)$ with $\tau_1 = 1,2,...,L_1 = (N_1 + \bar{N}_1)/d$ by the bit grouping block with $\bar{N}_1$ being the number of dummy bits. After that, the SM mapper generates the $N_\mathrm{T} \times 1$ transmission vector denoted as

$$\mathbf{c}^S_{m_1,a_1}(\tau_1) = [...,0,c^S_{m_1}(\tau_1),0,...]^\mathrm{T} \tag{13}$$

where $c^S_{m_1}(\tau_1)$ is the modulated symbol, $m_1 \in \{1,2,...,M\}$ and $a_1(\tau_1) \in \{1,2,...,N_\mathrm{T}\}$. Next, the transmission vector $\mathbf{c}^S_{m_1,a_1}(\tau_1)$ is sent towards the destination and relay nodes, respectively. The destination node receives signal sequence $\mathbf{z}_{S,D}(\tau_1) \in \mathbb{C}^{N_\mathrm{R}\times 1}$ given by

$$\begin{aligned}\mathbf{z}_{S,D}(\tau_1) &= \mathbf{H}_{S,D}\mathbf{c}^S_{m_1,a_1}(\tau_1) + \mathbf{n}_{S,D}(\tau_1) \\ &= \mathbf{h}^{a_1(\tau_1)}_{S,D} c^S_{m_1}(\tau_1) + \mathbf{n}_{S,D}(\tau_1)\end{aligned} \tag{14}$$

where $\mathbf{H}_{S,D} \in \mathbb{C}^{N_\mathrm{R}\times N_\mathrm{T}}$ represents the channel matrix from source to destination, $\mathbf{h}^{a_1(\tau_1)}_{S,D} \in \mathbb{C}^{N_\mathrm{R}\times 1}$ is the fading vector, and $\mathbf{n}_{S,D}(\tau_1) \in \mathbb{C}^{N_\mathrm{R}\times 1}$ is source to destination noise vector. $\mathbf{H}_{S,D}$, $\mathbf{h}^{a_1(\tau_1)}_{S,D}$ and $\mathbf{n}_{S,D}(\tau_1)$ are defined like $\mathbf{H}$, $\mathbf{h}^{a(\tau)}$ and $\mathbf{n}(\tau)$ in (7), respectively. Likewise, the relay gets the $\mathbf{z}_{S,R}(\tau_1) \in \mathbb{C}^{N_\mathrm{T}\times 1}$ written as

$$\begin{aligned}\mathbf{z}_{S,R}(\tau_1) &= \mathbf{H}_{S,R}\mathbf{c}^S_{m_1,a_1}(\tau_1) + \mathbf{n}_{S,R}(\tau_1) \\ &= \mathbf{h}^{a_1(\tau_1)}_{S,R} c^S_{m_1}(\tau_1) + \mathbf{n}_{S,R}(\tau_1)\end{aligned} \tag{15}$$

where $\mathbf{H}_{S,R} \in \mathbb{C}^{N_\mathrm{T}\times N_\mathrm{T}}$, $\mathbf{h}^{a_1(\tau_1)}_{S,R} \in \mathbb{C}^{N_\mathrm{T}\times 1}$ and $\mathbf{n}_{S,R}(\tau_1) \in \mathbb{C}^{N_\mathrm{T}\times 1}$ are defined similarly as $\mathbf{H}_{S,D}$, $\mathbf{h}^{a_1(\tau_1)}_{S,D}$ and $\mathbf{n}_{S,D}(\tau_1)$ in (14), respectively.

In time slot-2, the SM demapper performs demodulation for the received signal $\mathbf{z}_{S,R}(\tau_1)$ and gives rise to the soft LLR sequence $\mathbf{\Psi}_{S,R}(\mathbf{c}^S(\tau_1))$ which is fed into the bit ungrouping to get $\mathbf{\Psi}_{S,R}(\mathbf{c}^S)$. The QC-LDPC$_1$ decoding is then performed to generate the estimate $\hat{\mathbf{c}}'^S$ of $\mathbf{c}'^S$. The QC-LDPC$_2$ encoding block with the parity-check matrix $\mathbf{H}_2 = [\mathbf{D}_1, \mathbf{D}_2, \mathbf{I}]$ encodes the sequence $\hat{\mathbf{c}}'^S$ and produces the parity-check sequence $\mathbf{c}'^R$ of length $(m_\mathrm{b} - 4)Z$. Through the puncturing block, we obtain the sequence $\mathbf{c}^R$ with length $N_2 = N - K - 2Z$, i.e., the parity part-2 exhibited in Fig. 3. Similar to (13), the $N_\mathrm{T} \times 1$ transmission vector generated at the relay is written as the following form:

$$\mathbf{c}^R_{m_2,a_2}(\tau_2) = [...,0,c^R_{m_2}(\tau_2),0,...]^\mathrm{T} \tag{16}$$

where $\tau_2 = 1,2,...,L_2 = (N_2 + \bar{N}_2)/d$, $c^R_{m_2}(\tau_2)$ stands for the modulated symbol, $m_2 \in \{1,2,...,M\}$ and $a_2(\tau_2) \in \{1,2,...,N_\mathrm{T}\}$. At the destination, the signal sequence $\mathbf{z}_{R,D}(\tau_2) \in \mathbb{C}^{N_\mathrm{R}\times 1}$ is expressed as

$$\begin{aligned}\mathbf{z}_{R,D}(\tau_2) &= \mathbf{H}_{R,D}\mathbf{c}^R_{m_2,a_2}(\tau_2) + \mathbf{n}_{R,D}(\tau_2) \\ &= \mathbf{h}^{a_2(\tau_2)}_{R,D} c^R_{m_2}(\tau_2) + \mathbf{n}_{R,D}(\tau_2)\end{aligned} \tag{17}$$

where $\mathbf{H}_{R,D} \in \mathbb{C}^{N_\mathrm{R}\times N_\mathrm{T}}$, $\mathbf{h}^{a_2(\tau_2)}_{R,D} \in \mathbb{C}^{N_\mathrm{R}\times 1}$ and $\mathbf{n}_{R,D}(\tau_2) \in \mathbb{C}^{N_\mathrm{R}\times 1}$ are defined like $\mathbf{H}_{S,D}$, $\mathbf{h}^{a_1(\tau_1)}_{S,D}$ and $\mathbf{n}_{S,D}(\tau_1)$ in (14). Finally, we employ the joint QC-LDPC decoding to decode the combined LLR sequence $\mathbf{\Psi}(\bar{\mathbf{c}}) = [\mathbf{\Psi}_{S,D}(\mathbf{c}^S), \mathbf{\Psi}_{R,D}(\mathbf{c}^R)]$ of $\mathbf{\Psi}_{S,D}(\mathbf{c}^S)$ and $\mathbf{\Psi}_{R,D}(\mathbf{c}^R)$ from the source and relay, respectively, to get the estimated sequence $\hat{\mathbf{u}}'$.

5. Performance Analysis for the Proposed Schemes

This section analyses the theoretical performance of the proposed QC-LDPCC-SM and D-QC-LDPCC-SM schemes over quasi-static Rayleigh fading channel. The average error probability of the D-QC-LDPCC-SM scheme in cooperative scenarios can be derived from that of non-cooperative QC-LDPCC-SM scheme.

5.1 Performance Analysis for the QC-LDPCC-SM Scheme

Firstly, we derive the theoretical performance for the non-cooperative QC-LDPCC-SM scheme. The literature [9], [18] has defined the bit error probability (BEP) p_{b} for any linear binary code. Therefore, for the (N, K) QC-LDPC code, it can be mathematically written as

$$p_{\mathrm{b}} = \sum_{w=d_{\min}}^{N} \frac{A_w}{K} p(\mathbf{X} \to \hat{\mathbf{X}}) \tag{18}$$

where $d_{\min}$ stands for the minimum distance of the code and A_w represents the number of codewords of weight w determined by the simulations. $p(\mathbf{X} \to \hat{\mathbf{X}})$ denotes the unconditional error probability (UEP) committed by selecting the mapped coded SM symbol block $\mathbf{X} = [\mathbf{c}_{m,a}(1), \mathbf{c}_{m,a}(2), ..., \mathbf{c}_{m,a}(L)]$ instead of $\hat{\mathbf{X}} = [\hat{\mathbf{c}}_{m,a}(1), \hat{\mathbf{c}}_{m,a}(2), ..., \hat{\mathbf{c}}_{m,a}(L)]$. By employing the method in [18], the UEP of the proposed non-cooperative scheme is given by

$$p(\mathbf{X} \to \hat{\mathbf{X}}) = \frac{1}{\pi} \int_0^{\pi/2} M_{\gamma_{S,D}} \left(-\frac{1}{2\sin^2 \theta} \right) \mathrm{d}\theta \tag{19}$$

where $M_{\gamma_{S,D}}(g)$ denotes the moment generating function (MGF) of

$$\gamma_{S,D} = \frac{\chi_{S,D}}{2} \| \mathbf{H}(\mathbf{X} - \hat{\mathbf{X}}) \|_{\mathrm{F}}^2 \tag{20}$$

where $\chi_{S,D}$ represents the signal-to-noise ratio (SNR). The integral of (19) is maximum when $\sin^2 \theta = 1$, thus, the upper bound is

$$p(\mathbf{X} \to \hat{\mathbf{X}}) \le \frac{1}{2} M_{\gamma_{S,D}} \left(-\frac{1}{2} \right). \tag{21}$$

For quasi-static Rayleigh fading channel, we use a known result from the theory of multivariate Gaussian distributions (see [19]) as the MGF. Substitute (21) into (18), and we get the BEP bound of the QC-LDPCC-SM.

5.2 Performance Analysis for the D-QC-LDPCC-SM Scheme

Now, we discuss the BEP of the proposed D-QC-LDPCC-SM scheme in cooperative scenarios. For the convenience of analysis, let the *S*-*R* link be ideal. As such, we only need to consider the two independent channels, i.e., *S*-*D* and *R*-*D* channels. By multiplying the MFG functions $M_{\bar{\gamma}_{S,D}}(g)$ and $M_{\bar{\gamma}_{R,D}}(g)$ of the two links, the total MGF of the D-QC-LDPCC-SM is then obtained, and represented as

$$M_{\bar{\gamma}}^{\mathrm{coop}}(g) = M_{\bar{\gamma}_{S,D}}(g) \times M_{\bar{\gamma}_{R,D}}(g) \tag{22}$$

where $\bar{\gamma}_{S,D}$ and $\bar{\gamma}_{R,D}$ are mathematically denoted as

$$\bar{\gamma}_{S,D} = \frac{\chi_{S,D}}{2} \| \mathbf{H}_{S,D}(\mathbf{X}_1 - \hat{\mathbf{X}}_1) \|_{\mathrm{F}}^2, \tag{23}$$

$$\bar{\gamma}_{R,D} = \frac{\chi_{R,D}}{2} \| \mathbf{H}_{R,\mathrm{D}}(\mathbf{X}_2 - \hat{\mathbf{X}}_2) \|_{\mathrm{F}}^2. \tag{24}$$

In (23) and (24), $\mathbf{X}_1 = [\mathbf{c}_{m_1,a_1}^S(1), \mathbf{c}_{m_1,a_1}^S(2), ..., \mathbf{c}_{m_1,a_1}^S(L_1)]$ and $\mathbf{X}_2 = [\mathbf{c}_{m_2,a_2}^R(1), \mathbf{c}_{m_2,a_2}^R(2), ..., \mathbf{c}_{m_2,a_2}^R(L_2)]$ are the coded SM symbol blocks at the *S* and *R*, respectively. Furthermore, $\hat{\mathbf{X}}_1 \neq \mathbf{X}_1$ and $\hat{\mathbf{X}}_2 \neq \mathbf{X}_2$.

After using the mathematical manipulations, the total UEP of the D-QC-LDPCC-SM is given by

$$p_{\mathrm{coop}}(\mathbf{X} \to \hat{\mathbf{X}}) = \frac{1}{\pi} \int_0^{\pi/2} M_{\bar{\gamma}_{S,D}} \left(-\frac{1}{2\sin^2 \theta} \right) M_{\bar{\gamma}_{R,D}} \left(-\frac{1}{2\sin^2 \theta} \right) \mathrm{d}\theta. \tag{25}$$

By assuming $\sin^2 \theta = 1$, the upper bound of (25) is

$$p_{\mathrm{coop}}(\mathbf{X} \to \hat{\mathbf{X}}) \le \frac{1}{2} M_{\bar{\gamma}_{S,D}} \left(-\frac{1}{2} \right) M_{\bar{\gamma}_{R,D}} \left(-\frac{1}{2} \right). \tag{26}$$

The final BEP bound of the proposed D-QC-LDPCC-SM scheme can be measured by substituting (26) in (18), i.e.,

$$p_{\mathrm{b}} = \sum_{w=d_{\min}}^{N} \frac{A_w}{K} p_{\mathrm{coop}}(\mathbf{X} \to \hat{\mathbf{X}}). \tag{27}$$

In above description, the *R* is always in cooperation since we assume the *S*-*R* channel is ideal. However, in the case of non-ideal *S*-*R* link, the average of *S*-*D*, *S*-*R* and *R*-*D* channels is viewed as the overall probability [6].

6. Simulation Results

The simulated results about the proposed schemes are discussed in this section. For a fair comparison, the coded cooperative and non-cooperative systems keep an identical code rate, i.e., $R_{\mathrm{c}} = 1/3$ from the destination point of view. The information length $K = 4096$ and the lifting size $Z = 192$ are used. Furthermore, the ''min-sum'' algorithm with 50 iterations is used to decode LDPC codes. The SNR between the *S*-*R* link is represented as $\chi_{S,R}$. Similarly, $\chi_{S,D}$ and $\chi_{R,D}$ are the SNRs of the *S*-*D* and *R*-*D* links, respectively. As compared to the source node, the relay node is deployed closer to the destination node. Therefore, we assume that a 1 dB SNR gain is given by the relay node, i.e., $\chi_{R,D} = \chi_{S,D} + 1$.

6.1 Comparison of Theoretical and Simulated Results for the Proposed QC-LDPCC-SM and D-QC-LDPCC-SM Schemes

In this subsection, we compare the theoretical and simulated results of the proposed QC-LDPCC-SM and D-QC-LDPCC-SM schemes, as shown in Fig. 5. In the simulation, the ideal source-to-relay channel ($\chi_{S,R}=\infty$) and quasi-static Rayleigh fading channel are assumed. It can be observed that their BER performances well agree with the corresponding theoretical results at high SNR, which validates the effectiveness of the proposed theoretical analytical frameworks. Furthermore, we notice that the proposed D-QC-LDPCC-SM scheme in cooperative scenarios outperforms the non-cooperative QC-LDPCC-SM scheme under identical conditions. For instance, at a BER of 5×10^{-7}, the D-QC-LDPCC-SM scheme gains about 1.25 dB in SNR over the QC-LDPCC-SM scheme. This can be attributed to the following two key points: a) The additional SNR gain given to the relay node helps the correct decoding of information sequence from the source node. b) At the destination, the joint QC-LDPC decoding is exploited to jointly decode the LDPC code.

6.2 Performance Comparison of the QC-LDPCC-SM and D-QC-LDPCC-SM with the Existing Systems

This subsection compares their error performance of proposed systems with the existing multi-level polar coded non-cooperative and cooperative SM systems over quasi-static Rayleigh fading channel in [15], i.e., MLPC-SM and MLPCC-SM. The MLPC-SM and MLPCC-SM are used as the benchmarks for QC-LDPCC-SM and D-QC-LDPCC-SM, respectively. As observed from Fig. 6, the proposed QC-LDPCC-SM scheme performs better than the MLPC-SM scheme under the same conditions such as $N_{\mathrm{T}}=8$, $N_{\mathrm{R}}=4$ and 16-QAM. The superiority of the D-QC-LDPCC-SM scheme ($\chi_{S,R}=\infty$) over the MLPCC-SM scheme me is also exhibited in Fig. 6. The reason behind such an enticing gain is that the existing scheme utilizes successive cancellation polar decoding which is devoid of iterations. Furthermore, the existing scheme is not optimized for fading channel as the selection of channel capacities is based on heuristic approach.

6.3 Performance Comparison of the Systems Based on Different Fading Channel Models

In the wireless channel of the system, the fading is the finite multipath fading. Two fading channel models, i.e., the quasi-static Rayleigh fading channel model $\mathbf{H}$ and Rician fading channel model [15] $\mathbf{H}_{\mathrm{Ric}}=\sqrt{K_{\mathrm{Ric}}/(1+K_{\mathrm{Ric}})}\bar{\mathbf{H}}+\sqrt{1/(1+K_{\mathrm{Ric}})}\mathbf{H}$ are used to analyze the system error performance under the wireless

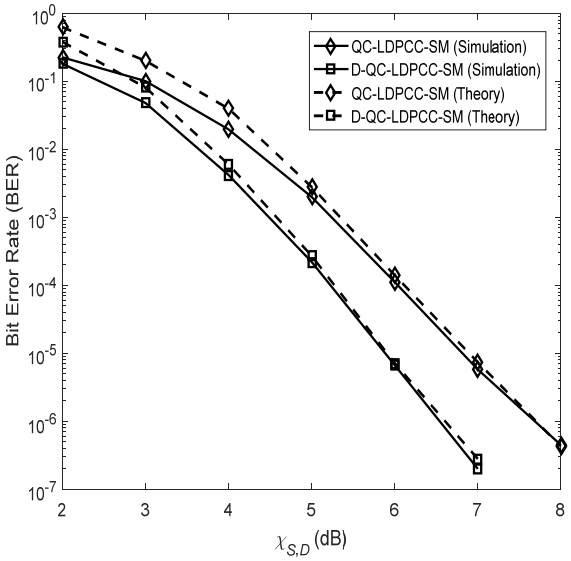

Fig. 5. Performance comparison for theoretical and simulation results of the proposed schemes, $N_{\mathrm{T}}=8$, $N_{\mathrm{R}}=4$ and 16-QAM.

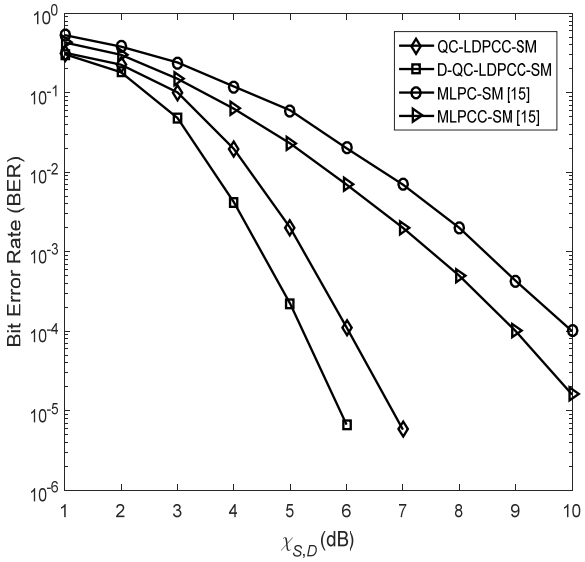

Fig. 6. Performance comparison for the proposed schemes with the existing schemes.

channel, where K_{Ric} is the Rician factor and $\bar{\mathbf{H}}$ denotes an all one matrix. Figure 7 exhibits the performance curves of the non-cooperative uncoded system (without SM) utilizing a single antenna at each node, where BPSK is used. The results reveal that the performance based on the Rician fading channel model (with $K_{\mathrm{Ric}}=2$) is better than that based on the Rayleigh fading channel model. Thus, this shows that the Rician fading channel model could be the better to describe the wireless channel of the system. Moreover, Figure 8 demonstrates the impact of this channel on the performance of the proposed schemes. Observe in Fig. 8 that the QC-LDPCC-SM and D-QC-LDPCC-SM ($\chi_{S,R}=\infty$) schemes based on the Rician fading channel model outperform those based on the Rayleigh fading channel model, respectively. For instance, the D-QC-LDPCC-SM scheme under the Rician fading channel model

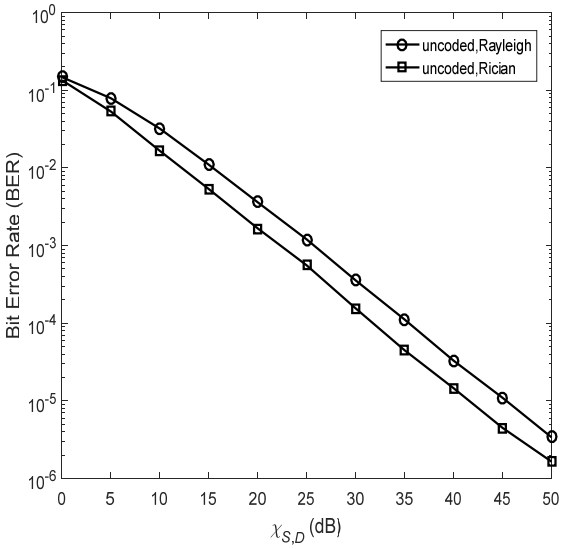

Fig. 7. Performance of the non-cooperative uncoded system without SM based on different fading channel models.

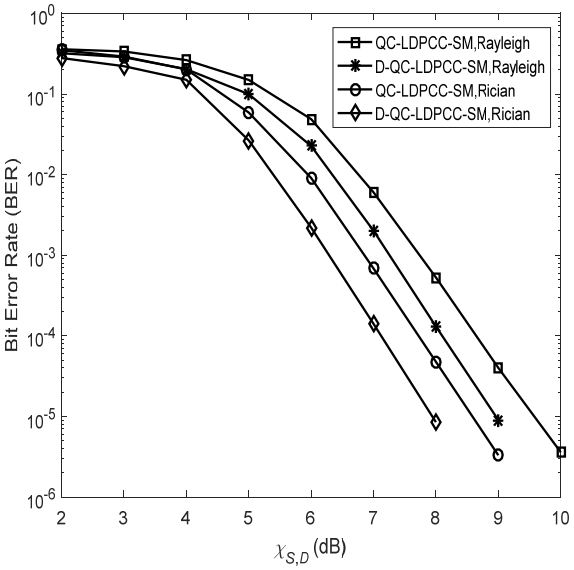

Fig. 8. Performance of the proposed schemes based on different fading channel models, N_T=8, N_R=3 and 16-QAM.

gains about 1 dB over that under the Rayleigh fading channel model at BER = 1×10^{-5}.

6.4 Performance Comparison of the D-QC-LDPCC-SM Scheme under Non-Ideal and Ideal Source-to-Relay Links

Figure 9 presents the BER performance of the D-QC-LDPCC-SM scheme over quasi-static Rayleigh fading channel with different modulation techniques in the case of non-ideal ($\chi_{S,R} \neq \propto$) and ideal ($\chi_{S,R} = \propto$) source to relay channels. For each digital modulation scheme, the error performance of the non-ideal D-QC-LDPCC-SM scheme is close to that of the ideal D-QC-LDPCC-SM scheme if the source-to-relay link is excellent. Specifically, for 16-QAM, the D-QC-LDPCC-SM scheme under $\chi_{S,R} = 5$ dB is only 0.2 dB worse than that under the ideal link. For 32-QAM and 64-QAM, the non-ideal cases ($\chi_{S,R} = 6$ dB and 8 dB) only lag behind by approximately 0.21 dB and 0.22 dB over their corresponding ideal cases, respectively. However, if the source-to-relay link under each modulation technique gets poor, i.e., $\chi_{S,R} = 2$ dB under 16-QAM, $\chi_{S,R} = 3$ dB under 32-QAM, and $\chi_{S,R} = 4$ dB under 64-QAM, the achievable error performance is degraded and the scheme exhibits an early error floor. This is because incorrect decoding at the relay leads to error propagation. Moreover, Figure 9 illustrates that as the modulation order grows, a noticeable performance loss is generated. The behavior can be explained that higher order modulation is more sensitive against the bit errors, which causes the performance degradation as a result.

6.5 Performance of the Proposed Schemes with Perfect and Imperfect CSI

In subsections 6.1–6.4, the perfect CSI is assumed. Here we present the error performance about the QC-LDPCC-SM and D-QC-LDPCC-SM ($\chi_{S,R} = \propto$) employing 16-QAM with the imperfect CSI under quasi-static Rayleigh fading channel. In non-cooperative scenarios, the parameters $L = 1756$, $J = 439$, $T = L/J = 4$ and $I_{itr} = 6$ are used to estimate the CSI. For a fair comparison, we utilize the parameters ($L = 640$, $J = 160$, $T = L/J = 4$, $I_{itr} = 6$) and ($L = 1116$, $J = 279$, $T = L/J = 4$, $I_{itr} = 6$) to estimate the *S-D* and *R-D* channels, respectively. From Fig. 10, it can be observed that the QC-LDPCC-SM scheme using the IJCEDD-VBL closely approaches the QC-LDPCC-SM using the perfect CSI. Furthermore, in cooperative scenarios, we need to estimate the *S-D* and *R-D* links. However, the performance loss under imperfect CSI is within accepta-

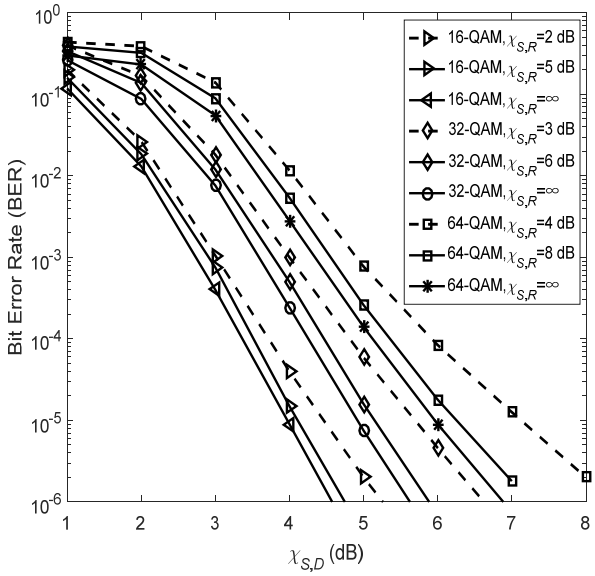

Fig. 9. BER performance of the D-QC-LDPCC-SM scheme with different modulation techniques under $\chi_{S,R} = \propto$ and $\chi_{S,R} \neq \propto$, $N_T = 8$ and $N_R = 5$.

ble range compared to the performance of a perfect-CSI scenario. Thus, this validates the effectiveness of the proposed IJCEDD-VBL scheme. Moreover, the numerical results demonstrate that the proposed IJCEDD-VBL outperforms the existing IJCEDD scheme [17], where the performance gap is about 0.4 dB at BER = 5×10^{-5}.

In addition, we present the error performance of the proposed QC-LDPCC-SM scheme under the imperfect CSI with various number of iterations (i.e., $I_{\text{itr}} = 1$, 2, 3, 4, 5 and 6). For estimating the CSI, the parameters $L = 1756$, $J = 439$ and $T = L/J = 4$ are used. The simulation results in Fig. 11 demonstrate that the system error performance is improved as the iteration number increases. However, the performance with $I_{\text{itr}} > 3$ changes very little as compared to the performance with $I_{\text{itr}} = 3$. Thus, an optimal value for the iteration number for Algorithm 1 is $I_{\text{itr}} = 3$. Moreover, the convergence behavior of the system error performance is also exhibited in the simulation results. Observe in Fig. 11 that the system error performance starts to converge over the whole SNR when $I_{\text{itr}} = 2$.

6.6 Performance Comparison of the QC-LDPCC-SM Scheme and Other Schemes

In the previous subsections of this section, the uncorrelated channel is assumed. In fact, the presence of local scatterers and insufficient antenna spacing will result in spatial correlation between the transmitting and receiving antennas. Therefore, the performance of the QC- LDPCC-SM scheme over correlated Rayleigh fading channel under perfect CSI is also analyzed. The correlated fading channels can be mathematically modelled by $\mathbf{H}_{\text{corr}} = \mathbf{Z}_{\text{R}}^{1/2}\mathbf{H}\mathbf{Z}_{\text{T}}^{1/2}$ with $\mathbf{Z}_{\text{R}} = [z_{p,q}]_{N_{\text{R}} \times N_{\text{R}}}$ and $\mathbf{Z}_{\text{T}} = [z_{p,q}]_{N_{\text{T}} \times N_{\text{T}}}$ being the spatial correlation matrices at the receiver and transmitter, respectively. During the simulations, $z_{p,q} = z^{*}_{p,q} = z^{|q-p|}$ with $(\cdot)^{*}$ denoting complex conjugation and z being the amount of correlation having $|z| < 1$ [12]. System error performance using 16-QAM under correlated ($z = 0.4$ and 0.8) and uncorrelated ($z = 0$) channels is exhibited in Fig. 12. As illustrated in simulation results, the spatial correlation greatly affects the performance of the QC-LDPCC-SM scheme. Specifically, when compared to the QC-LDPCC-SM scheme over uncorrelated channel conditions, the QC-LDPCC-SM scheme under correlated channel conditions suffers from a substantial performance degradation.

Furthermore, the performance comparison between the proposed scheme and the turbo coded SM (TC-SM) scheme using different interleavers (i.e., the random and *S*-random interleavers [20]) is also performed under identical conditions. In the TC-SM scheme, the turbo encoder contains two identical recursive systematic convolutional (RSC) encoders and an interleaver. Each RSC encoder has the generator matrix $\mathbf{G} = [1,5/7]_8$. Also, the turbo decoder with soft out Viterbi algorithm (SOVA) uses eight iterations (the optimal number of decoding iterations is eight) to recover the source information. From Fig. 12, we observe

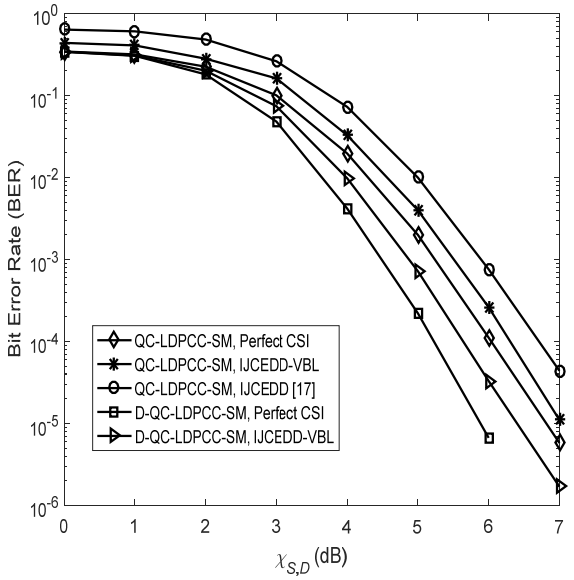

Fig. 10. Performance of proposed schemes with the perfect and imperfect CSI, 16-QAM, $N_{\text{T}} = 8$ and $N_{\text{R}} = 4$.

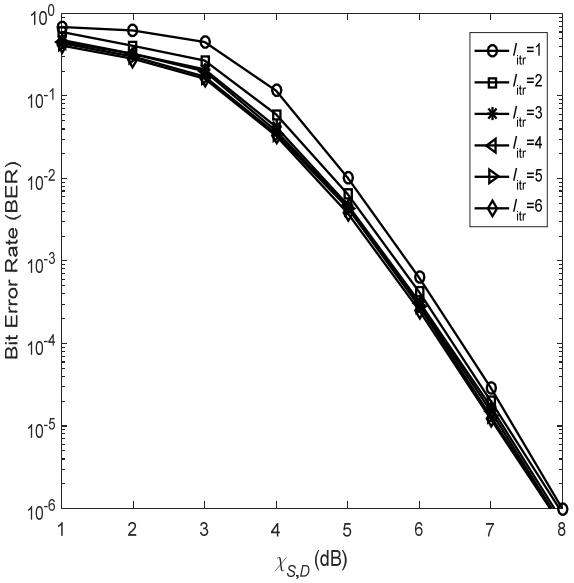

Fig. 11. Performance comparison of the QC-LDPCC-SM scheme under the imperfect CSI with various number of iterations, 16-QAM, $N_{\text{T}} = 8$ and $N_{\text{R}} = 4$.

that the QC-LDPCC-SM scheme ($z = 0.4$) has a better BER performance compared with the TC-SM scheme using different interleavers. For example, for the TC-SM scheme, the system performances with the random and *S*-random interleavers are separately 1.8×10^{-5} and 5.6×10^{-6} at SNR = 9 dB. However, at the same SNR, the QC-LDPCC-SM scheme ($z = 0.4$) demonstrates excellent performance, i.e., 1.6×10^{-6}. Thus, this exhibits the superiority of our proposed scheme in comparison to its counterparts.

7. Conclusion

We propose the QC-LDPCC-SM scheme in this manuscript. To validate the efficacy of coded cooperation,

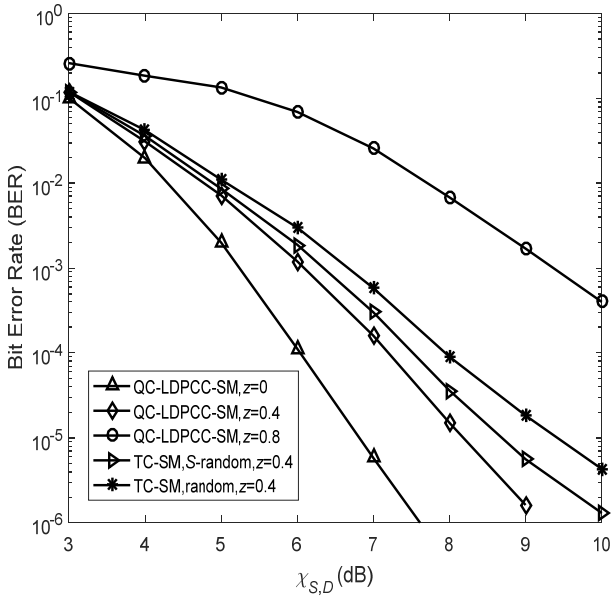

Fig. 12. Performance for the QC-LDPCC-SM and TC-SM schemes, 16-QAM, $N_T = 8$ and $N_R = 4$.

the D-QC-LDPCC-SM scheme as an extension of the QC-LDPCC-SM scheme is also presented. We derive the BER bound for the proposed schemes that verify the simulation results over quasi-static Rayleigh fading channel. Through Monte Carlo simulations, we observe the superiority of the D-QC-LDPCC-SM scheme compared to its non-cooperative counterpart. Also, the proposed schemes provide better error performance than the existing schemes. Moreover, we examine the proposed QC-LDPCC-SM and D-QC-LDPCC-SM schemes under the perfect and imperfect CSI. The numerical results show that the performance under the imperfect CSI generated by the proposed IJCEDD-VBL can approach the performance under the perfect CSI.

Acknowledgments

This work was supported by National Natural Science Foundation of China under the contract No. 61771241.

References

[1] NGUYEN, T. T. B., TAN, T. N., LEE, H. Efficient QC-LDPC encoder for 5G new radio. *Electronics*, 2019, vol. 8, no. 6, p. 1–15. DOI: 10.3390/electronics8060668

[2] LI, H., BAI, B., MU, X., et al. Algebra-assisted construction of quasi-cyclic LDPC codes for 5G new radio. *IEEE Access*, 2018, vol. 6, p. 50229–50244. DOI: 10.1109/ACCESS.2018.2868963

[3] NGUYEN, T. T. B., LEE, H. Low-complexity multi-mode multi-way split-row layered LDPC decoder for gigabit wireless communications. *Integration-the VLSI Journal*, 2019, vol. 65, p. 189–200. DOI: 10.1016/j.vlsi.2018.12.004

[4] UMAR, R., YANG, F. F., XU, H. J., et al. Multi-level construction of polar coded single carrier-FDMA based on MIMO antennas for coded cooperative wireless communication. *IET Communications*, 2018, vol. 12, no. 10, p. 1253–1262. DOI: 10.1049/iet-com.2017.1436

[5] EJAZ, S., YANG, F., XU, H. Split labeling diversity for wireless half-duplex relay assisted cooperative communication systems. *Telecommunication Systems*, 2020, vol. 75, no. 4, p. 437–446. DOI: 10.1007/s11235-020-00694-6

[6] HUNTER, T. E., NOSRATINIA, A. Diversity through coded cooperation. *IEEE Transactions on Wireless Communications*, 2006, vol. 5, no. 2, p. 283–289. DOI: 10.1109/TWC.2006.02006

[7] ZHANG, S. W., YANG, F. F., TANG, L., et al. Joint design of QC-LDPC codes for coded cooperation system with joint iterative decoding. *International Journal of Electronics*, 2015, vol. 103, no. 3, p. 384–405. DOI: 10.1080/00207217.2015.1036374

[8] MUGHAL, S., YANG, F. F., EJAZ, S., et al. Asymmetric turbo code for coded-cooperative wireless communication based on matched interleaver with channel estimation and multi-receive antennas at the destination. *RadioEngineering*, 2017, vol. 26, no. 3, p. 878–889. DOI: 10.13164/re.2017.0878

[9] MUGHAL, S., YANG, F. F., UMAR, R. Reed-Muller network coded-cooperation with joint decoding. *IEEE Communications Letters*, 2019, vol. 23, no. 1, p. 24–27. DOI: 10.1109/LCOMM.2018.2879101

[10] UMAR, R., YANG, F., MUGHAL, S., et al. Distributed polar-coded OFDM based on Plotkin's construction for half duplex wireless communication. *International Journal of Electronic*s, 2018, vol. 105, no. 7, p. 1097–1116. DOI: 10.1080/00207217.2018.1426118

[11] MESLEH, R. Y., HAAS, H., SINANOVIC, S., et al. Spatial modulation. *IEEE Transactions on Vehicular Technology*, 2008, vol. 57, no. 4, p. 2228–2241. DOI: 10.1109/TVT.2008.912136

[12] BASAR, E., AYGOLU, U., PANAYIRCI, E., et al. New trellis code design for spatial modulation. *IEEE Transactions on Wireless Communications*, 2011, vol. 10, no. 8, p. 2670–2680. DOI: 10.1109/TWC.2011.061511.101745

[13] ZHAO, C., YANG, F., UMAR, R., et al. Two-source asymmetric turbo-coded cooperative spatial modulation scheme with code matched interleaver. *Electronics*, 2020, vol. 9, no. 1, p. 1–20. DOI: 10.3390/electronics9010169

[14] ZHAO, C., YANG, F., WAWERU, D. K. Reed-Solomon coded cooperative spatial modulation based on nested construction for wireless communication. *RadioEngineering*, 2021, vol. 30, no. 1, p. 172–183. DOI: 10.13164/re.2021.0172

[15] MUGHAL, S., YANG, F., XU, H., et al. Coded cooperative spatial modulation based on multi-level construction of polar code. *Telecommunication Systems*, 2019, vol. 70, p. 435–446. DOI: 10.1007/s11235-018-0485-6

[16] CHEN, T., VAKILINIA, K., DIVSALAR, D., et al. Protograph-based Raptor-like LDPC codes. *IEEE Transactions on Communications*, 2015, vol. 63, no. 5, p. 1522–1532. DOI: 10.1109/TCOMM.2015.2404842

[17] SUGIURA, S., HANZO, L. Effects of channel estimation on spatial modulation. *IEEE Signal Processing Letters*, 2012, vol. 19, no. 12, p. 805–808. DOI: 10.1109/LSP.2012.2221707

[18] SIMON, M. K., ALOUINI, M. S. *Digital Communication over Fading Channels*. 2nd ed. New Jersey (USA): Wiley, 2005. ISBN: 0-471-64953-8

[19] SCHWARTZ, M., BENNETT, W. R., STEIN, S. *Communications Systems and Techniques*. New York: McGraw-Hill, 1966. ISBN: 0-7803-4715-3

[20] FENG, W., YUAN, J., VUCETIC, B. S. A code-matched interleaver design for turbo codes. *IEEE Transactions on Communications*, 2002, vol. 50, no. 6, p. 926–937. DOI: 10.1109/TCOMM.2002.1010612

About the Authors ...

Chunli ZHAO (corresponding author) received her B.S. degree in Electronic and Information Engineering from Henan Normal University Xinlian College, China, in 2014. She obtained her M.Sc. degree in Circuits and Systems at Henan Normal University, China, in 2017. She is currently doing Ph.D. from the College of Electronic and Information Engineering, Nanjing University of Aeronautics and Astronautics, China. Her research interests are circuits and systems, signal processing and channel coding.

Fengfan YANG received the M.Sc. and Ph.D. degrees from the Northwestern Polytechnical University and South-east University, China in 1993, and 1997, respectively, all in Electronic Engineering. He has been with the College of Information Science and Technology, Nanjing University of Aeronautics and Astronautics since May 1997. From October 1999 to May 2003, he was a research associate at the Centre for Communication Systems Research, University of Surrey, UK, and Dept. of Electrical and Computer Engineering, McGill University, Canada. His major research interests are information theory, channel coding and their applications for mobile and satellite communications.

Daniel Kariuki WAWERU received his B.Sc. degree in Mathematics and M.Sc. degree in Pure Mathematics from the University of Nairobi, Kenya, in 2015 and 2017. He is currently doing Ph.D. from the College of Electronic and Information Engineering, Nanjing University of Aeronautics and Astronautics, China. His research interests are coding theory, information theory, channel coding for wireless communications.

Chen CHEN received her B.S degree in Electronic and Information Engineering from Yangzhou University, China, in 2020. She is currently doing Ph.D. from the College of Electronic and Information Engineering, Nanjing University of Aeronautics and Astronautics, China. Her research interests are circuits and systems, signal processing and channel coding.

Hongjun XU (MIEEE, 07) received the B.Sc. degree from the University of Guilin Technology, Guilin, China, in 1984; the M.Sc. degree from the Institute of Telecontrol and Telemeasure, Shi Jian Zhuang, China, in 1989; and the Ph.D. degree from the Beijing University of Aeronautics and Astronautics, Beijing, China, in 1995. From 1997 to 2000, he was a Postdoctoral Fellow with the University of Natal, Durban, South Africa, and Inha University, Incheon, Korea. He is currently a full Professor with the School of Engineering at the University of KwaZulu-Natal, Durban. He is also a rated scientist of the national research foundation in South Africa. He has authored and co-authored more than 50 journal papers. His research interests include wireless communications and image processing.